Analysis of Fertilization Effects on Rice and Wheat by Time-Series Clustering of Vegetation Index Data

Taichi Ito [1], Ken'ichi Minamino [1] and Shintaro Umeki [2]

[1] *Graduate School of Software and Information Science, Iwate Prefectural University, 152-52 Sugo, Takizawa-shi, Iwate, 0200693, Japan*
[2] *Hanamaki branch, Research Center for Industrial Science and Technology, Iwate University, 5-6-3 Nimaibashi, Hanamaki-shi, Iwate, 0250312, Japan*

Abstract

Because the efficiency of farming in Japan largely depends upon personal experience, approaches toward farming are not frequently shared. To illustrate this tacit knowledge, the present study was conducted to visualize the fertilization effect via drone monitoring. Through continuous monitoring, we obtained time-series data of four vegetation indices in an approximately 3m mesh square grid, and employed clustering to analyze it. By performing such an analysis on paddy rice and wheat fields with and without comparative adjustment of the fertilizer amount, the appropriate fertilizer amount and variation in growth within the field were cleared. Although the vegetation indices are often used in drone monitoring, their values may be difficult to interpret. By monitoring data with respect to years, fields, and types of plants, we constructed and investigated an average time-series curve, thereby obtaining criteria associated with growth quality. Furthermore, we developed a prediction model of each index to clarify and narrow down the validity period of the fertilizer application.

Keywords

drone, monitoring, vegetation index, rice, wheat, machine learning, clustering, random forest

1. Introduction

The number of farmers in Japan has experienced a considerable decline due to aging and a decrease in the number of new farmers. One primary cause of this decline is the inherent ambiguity of effective farming techniques, which are largely rooted in farmers' personal experiences. In other words, these techniques represent tacit knowledge, which are difficult to pass on to others. It is therefore necessary to convert the underlying tacit knowledge into formal knowledge. Because current evaluation methods for farming techniques are generally based on harvest yield, they cannot be employed prior to the harvest. Furthermore, the harvest yield is not a comprehensive measure of efficacy for farming techniques. Consequently, smart agriculture, wherein robots, artificial intelligence (AI), and the Internet of Things (IoT) are employed to accurately and inexpensively evaluate farming techniques, has become an emerging research topic. One example of smart agriculture is drone monitoring. Variations in growth are known to be ubiquitous even in smaller fields such as those in Japan. An effective way of monitoring the growth of crops in small fields involves high-frequency and high-resolution drones. Because these drones are autopiloted, this method can be used safely and effectively, as demonstrated through prior studies [1]. However, monitoring results must be interpretable and applicable in practice for individual farmers [2]. Although prior studies have employed vegetation indices to monitor crop conditions [1, 3, 4, 7, 8, 18], these values cannot be directly associated with quality. Other approaches manage crops for high yield with the objective of reaching and maintaining predetermined target values of vegetation indices. However, these approaches demand the use of manual handheld sensors, making the process highly time- and resource-intensive [3].

The 5th International Symposium on Advanced Technologies and Applications in the Internet of Things (ATAIT 2023), August 28-29, 2023, Kusatsu, Japan
EMAIL: g231u003@s.iwate-pu.ac.jp (T. Ito); minamino@iwate-pu.ac.jp (K. Minamino); sumeki@iwate-u.ac.jp (S. Umeki)

The present study was therefore conducted to visualize and evaluate a fertilizer application of rice and wheat crops using vegetation indices in conjunction with machine learning. Consequently, the effectual observation period was narrowed down from the obtained vegetation indices and machine learning results.

2. Method

Details pertaining to the experimental environment are listed in Table 1. The farm fields were located in the inland central area of Iwate Prefecture (Okamizawa, Yuguchi-8, Yokokawame, Todoroki-3). The varieties in each field were “Hitomebore” and “Yumiazusa” for paddy rice, and “Ginganochikara” and “Yukichikara” for wheat. The mesh area (data acquisition unit) was an approximately 3-5m square. Monitoring was conducted from the time when crop leaves first covered the ground to immediately prior to harvest (paddy rice: July to September; wheat: April to June), under consideration of optimal weather conditions. The drone used for monitoring was a P4 Multispectral (Figure 1) [18]. In this survey, Yuguchi-8 and Todoroki-3 were varied by fertilizer amount with the corresponding fertilizer effect visualized. The nitrogen amount in fertilizer was, at Yuguchi-8, 2.8, 3.5, 4.2[gN/m^2] from the North. At Todoroki-3, 3.2[gN/m^2] were applied to the entire field until the second application and 0.9[gN/m^2] only the West after the third application (Table 1).

Table 1
Experimental farmfield

Farmfield name		Okamizawa	Yuguchi-8	Yokokawame	Todoroki-3
Variety		Paddy rice Hitomebore	 Yumiazusa	Wheat Ginganochikara	 Yukichikara
Number of Meshes		743	818	735	489
Date	*Planting*	May. 7th	Early May.	Sep. 26th	Sep. 30th
	Fertilizer application	(North) Jul. 24th (Center, South) 1st: Aug. 1st 2nd: Aug. 6th	Jul. 20th	1st: Apr. 12th 2nd: May. 10th	(Entire) 1st: Apr. 7th 2nd: May. 5th (Only West) 3rd: May. 24th 4th: May. 30th
	Earing	Aug. 3rd	Early Aug.	May. 15th	May. 10th
	Harvesting	Sep. 27th	Early Oct.	Jul. 7th	Jul. 1st-4th
Comparable value		N/A	Fertilizer amount [gN/m^2] North: 2.8 Center: 3.5 South: 4.2	N/A	Fertilizer amount [gN/m^2] Entire: 3.2 Only West: 0.9
Aerial photo.		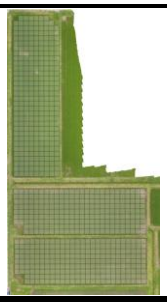	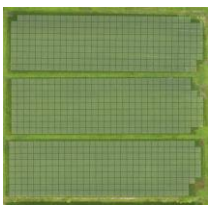		

Time-series data of vegetation indices for each mesh were obtained through continuous monitoring. Because no preliminary training data were present, unsupervised learning – specifically, the k-means clustering method – was employed to analyze these time-series data. Generally, clustering refers to the grouping of point data, as in the case of scatter plots. Because the present study was conducted on time-series data, clustering could not be performed directly. Instead, we employed a self-making function to cluster the data according to similar trends. Specifically, we adopted the TimeSeriesKmeans function of the tslearn module in Python [15]. The k-means method was used to determine the number of clusters subjectively using the elbow method.

Vegetation indices obtained from monitoring data are usually computed via sunlight reflex ratio of leaves. As shown in Figure 2, healthy crops exhibit a large difference in this ratio between the red and near-infrared (NIR) regions, whereas stressed crops show a smaller difference. Using these characteristics, we obtained the reflex ratios of three regions (Red, RedEdge, NIR), and evaluated the fertilizer application by three vegetation indices (NDVI, NDRE, CCCI) computed from these regions. The following subsections provide explanations for each vegetation index.

Figure 1: Drone used in this research (P4 Multispectral, DJI Co.)

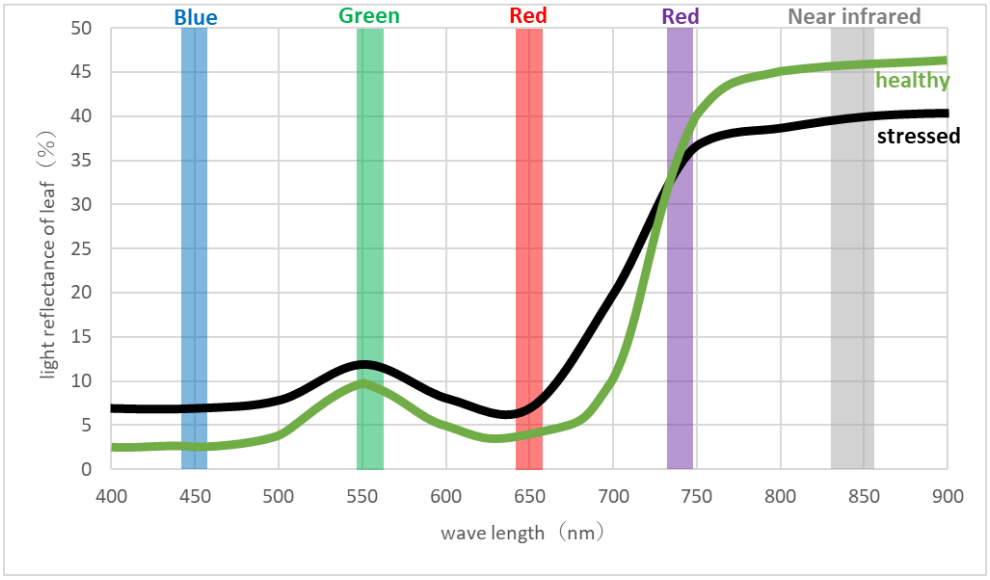

Figure 2: Spectral characteristics of leaf sunlight reflectivity

2.1. Normalized Difference Vegetation Index (NDVI)

This index, which diagnoses vegetation and harvest amount, is computed using reflex ratios in the Red and NIR regions as shown in Equation (1), taking a value between -1 and 1, wherein higher values indicate healthier vegetation [1]. This is one of the most common indices used to evaluate the growth of various plants.

$$NDVI = (NIR - Red)/(NIR + Red), \quad (1)$$

2.2. Normalized Difference RedEdge Index (NDRE)

This index, which diagnoses crop stress, ranges from -1 to 1 wherein higher values indicate less stress [4]. Its values are usually smaller than those of NDVI because RedEdge is closer to the NIR reflex ratio than Red (Figure 2). For paddy rice, NDRE is normally within a range of 0 – 0.3 [5]. It is difficult to identify the cause of stress looking solely at this index, and a subsequent field investigation is necessary. The results of such an investigation may reveal the following information according to when and where the stress level was raised [6]: There are holes in the ridges if values near the ridges are low; Root rot caused by floating straw if low on the leeward side; Overgrowth of weeds if low in July and August; Rice blast if low near the ridges at the end of August.

However, values of this index do not exhibit significant change in the absence of great stress. Accordingly, we employed an additional index (sNDRE: standardized NDRE) by standardizing the NDRE for each observation date [18].

$$NDRE = (NIR - RedEdge)/(NIR + RedEdge), \quad (2)$$

2.3. Canopy Chlorophyll Content Index (CCCI)

This index can diagnose the nitrogen content of crops. A related study used the CCCI to diagnose nitrogen ratios in wheat [7]. However, this index is not commonly used, and to our knowledge, no other studies have used it for rice.

The nitrogen content is calculated by the relationship equation between CCCI and the estimation formula of nitrogen content. The CCCI is computed via Equation (3). The $NDRE_{max}$ and $NDRE_{min}$ with the smallest root mean square error (RMSE) between the estimated and actual nitrogen contents are defined from the maximum and minimum lines, wherein all data are sandwiched in a two-dimensional plot of NDVI and NDRE [7, 8]. However, this index is computed by a simple method, as we could not collect actual nitrogen content. Here, $NDRE_{max}$ and $NDRE_{min}$ denote the maximum and minimum values of NDRE at a site on each monitoring date [9].

This index takes ranges 0 to 1 with higher values indicating higher nitrogen content. Because nitrogen is involved in the growth of crops as a component of fertilizers, CCCI can indicate the amount of nitrogen absorbed by the crops.

$$CCCI = (NDRE - NDRE_{min})/(NDRE_{max} - NDRE_{min}), \quad (3)$$

3. Field experiments

3.1. Diagnosis by Vegetation Indices for Each Field

The following subsections present clustering results of each site, as well as relationships between crop growth and vegetation indices. The clustering results and mesh distribution map are shown in Tables 2 and 3, respectively.

3.1.1. Okamizawa

This site was planted with a paddy rice called “Hitomebore.” Although no comparative experiments were conducted, the fertilization methods varied between the North and Center/South. At the North,

0.51[gN/m^2] were applied on July 24th. At the Center and South, farmer-made fertilizer was applied on August 1st and 6th.

In NDVI, the clusters were completely separated each field. Focusing on the earing period, the generated prediction was "lower harvest amount in the South because Cluster 2 was lower." In terms of NDRE, no significant stress was observed, as no low values were present throughout the monitoring period. In terms of sNDRE, overgrowth of weeds was predicted for the Center and South, as Cluster 2 exhibited a low score in August. In terms of CCCI, Cluster 1 exhibited an earlier peak than Clusters 0 and 2. These peaks represent the highest level of fertilizer efficiency on the crops, reflecting differences in fertilization between the North and Center/South regions.

3.1.2. Yuguchi-8

This site was used to conduct a comparative experiment with varying fertilizer amounts, wherein more fertilizer was used the further south you went. There were days when monitoring was not possible due to severe weather conditions.

In terms of NDVI, Clusters 0 and 3 were more desirable because their values were higher in the earing period. The North region, where fewer fertilizer was used, was predicted to yield the highest harvest amount. In terms of sNDRE, Cluster 2 exhibited a low value until the earing period. Because this value increased in August, no significant stress was diagnosed. In CCCI, the cluster distribution map indicated that the crops were classified in center and ridge regardless of fertilizer amount. This indicates that the fertilizer did not work consistently due to factors such as temperature and weather.

3.1.3. Yokokawame

This site was planted with a wheat called “Ginganochikara.” Because both fields onsite were worked identically, no comparative experiments were conducted [10].

Although the NDVI generally peaks at earing periods, this was not the case here. We presume that crop health was maintained by fertilizer application on April 12th, and monitoring could not proceed at the earing period. Cluster 0 exhibited good growth with high values throughout the monitoring period, whereas Clusters 1 and 2, which were located near the ridge, exhibited low values. In terms of sNDRE, Cluster 1 was associated with high stress. This may be explained by poor drainage, as the site was converted from a paddy rice field. Overall, these results indicate a need for soil improvement.

3.1.4. Todoroki-3

This site was planted with a wheat called “Yukichikara,” and comparative experiments were performed. As shown in Table 1, the West section was fertilized four times, whereas the East section was fertilized twice [10].

In terms of NDVI, the clustering distribution map shows that Cluster 0 was located in the West, Clusters 1 and 2 were in the East, and Cluster 3 represented the ridge. With the exception of Cluster 3, differences were observed from May 25th. Values for Cluster 1 exhibited a gradual decline, with a significant difference with those of Cluster 0 observed on June 15th. Considering that the third fertilizer application was on May 24th, this incongruity was assumed to be caused by variability in fertilizer amount. Thus, the combination of NDVI and machine learning could be used to visualize the fertilization effect on crops in a comparative manner. In other vegetation indices, the clusters were divided between the West and East sections. Particularly in terms of sNDRE, the East section exhibited low values from late May, indicating clear stress. From this, a prediction could be made: either the fertilization method used in the West section was more appropriate, or further steps can be made to minimize stress on crops.

Table 2
Results of time-series clustering

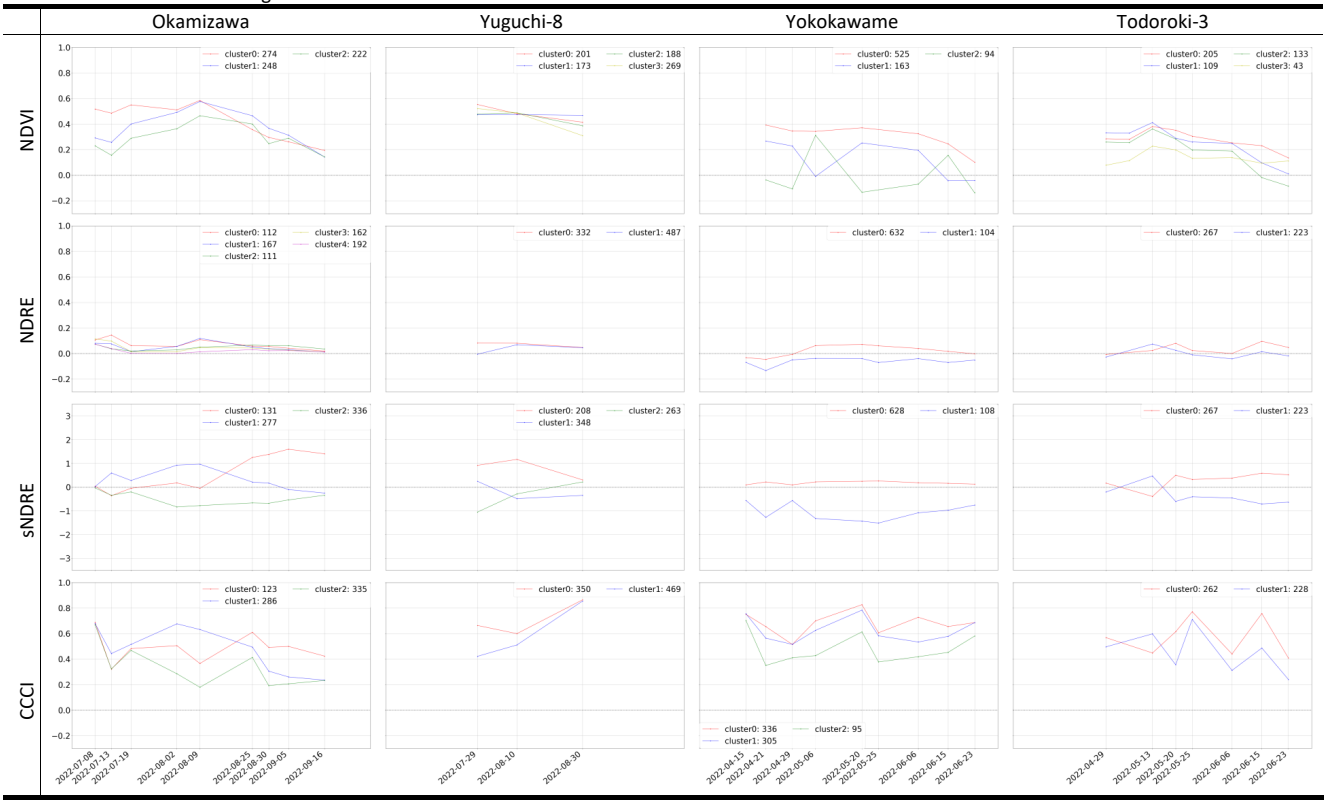

Table 3
Mesh distribution map

	Okamizawa	Yuguchi-8	Yokokawame	Todoroki-3
NDVI	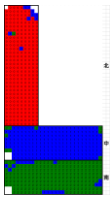	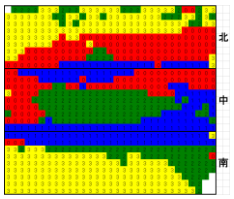	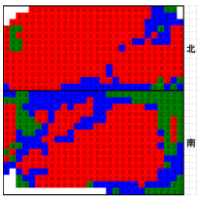	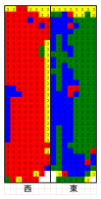
NDRE	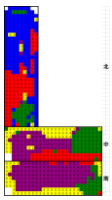	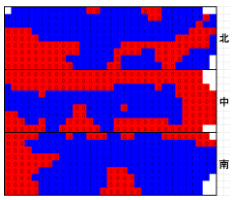	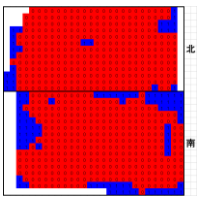	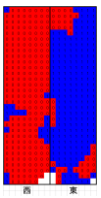
sNDRE	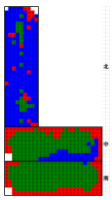	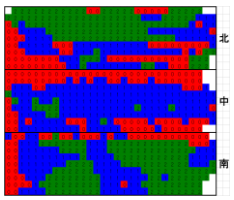	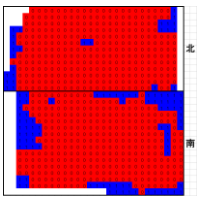	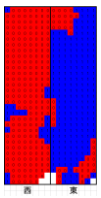
CCCI	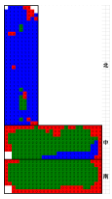	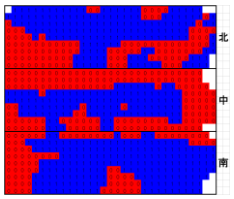	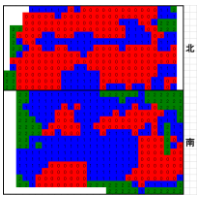	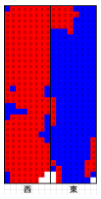

3.2. Diagnostic Criteria of Vegetation Indices

Our experimental results were used to interpret crop growth, stress level, fertilizer effects, and related factors according to time-series vegetation indices. In this section, growth comparison beyond location and year, as well as normal changes in each index, are explained based on the results of the 2021 work [9, 18] and the present study.

In terms of NDVI, all crops and sites exhibited a mountain pattern that peaked at the earing period. The peak values were approximately 0.6 for paddy rice and 0.4 for wheat. For paddy rice, optimal values of this index can be determined through multi-year monitoring. Specifically, clusters that have not exhibited bad growth were associated with values of at least 0.2 in early July, 0.4 in mid-July, and 0.6 at the earing period. No target values were recorded following the earing period because the harvest amount is typically determined here.

In terms of NDRE, a non-negative value indicates the absence of significant stress regardless of crop. sNDRE is more appropriate when visualizing small or relative stress, as it corresponds to changes in data under different monitoring conditions on the same scale. Note that a sNDRE of 0.0 represents average stress in a field.

Owing to the simple computation method used in this study, CCCI and sNDRE exhibited a relationship of normalization and standardization. Consequently, although the time series exhibited different degrees of variability, the distribution maps were somewhat similar. CCCI data from different years or locations could not be compared, as $NDRE_{max}$ and $NDRE_{min}$ vary from field to field whereas all CCCI values lie between 0.0 and 1.0.

4. Discussion

As described above, time-series clustering can help clarify differences in crop growth and fertilization effects. However, even though the drones are autopiloted, the monitoring process itself is not fully automated, with certain tasks, such as flight route setting, still requiring manual labor. To ensure monitoring efficiency, it is desirable to minimize the number of monitoring operations. To determine which observation date would yield the best result, we employed vegetation indices from "Okamizawa," as their field has a large quantity of observations and a relatively large difference between clusters, as shown in Tables 1, 2, and 3.

First, correlations between vegetation index values were calculated to analyze whether the efficient observation date differs for each vegetation index. These correlations were measured by the Spearman correlation coefficient [19], where D' is an arbitrary subset from all observation dates D, C is the number of clusters, X is the clustering result corresponding to D' and C, and Y is the set of all other clustering results. The similarity $dist$ between X and Y is then calculated using the following formula.

$$dist = \sum_{c \in C} \sum_{d \in D' \subset D} \sum_{i=1}^{n_c} \left(x_{c,d,i} - y_{c,d}\right)^2$$

where n_c is the number of meshes classified into cluster c in X, $x_{c,d,i}$ is the i-th mesh in cluster c in X on observation date d, and $y_{c,d}$ is the centroid value of cluster c in Y on observation date d. Thus, 510 dist values were computed excluding anomalies and outliers. These values were ranked in ascending order for each vegetation index, to calculate the Spearman correlation coefficients between vegetation indices, as listed in Table 4. Because no significant correlations were found between any indices, the effectual observation period was determined to differ for each vegetation index.

The random forest algorithm is frequently used in agricultural applications, such as harvest yield prediction and crop classification [16, 17]. We performed random forest to determine which observation date was important when classifying meshes. The vegetation index values of each observation date were set as independent variables whereas the cluster IDs were considered dependent variables. Approximately 25% of all 743 meshes were allocated as training data, with the remaining 75% used as test data. We evaluated the prediction accuracy of dependent variables within the test data using the decision tree generated from the training data. The random forest was implemented with the RandomForestClassifier module in Python [11], and the decision tree was visualized using Graphviz [12] and PyDotPlus [13]. The accuracy rates were approximately 98%, 84%, 95%, and 97% for NDVI, NDRE, sNDRE, and CCCI, respectively.

We observe that cluster IDs were classified very accurately with a small volume of training data for most vegetation indices. Only NDRE exhibited a slightly lower correct answer rate, as minimal differences were observed between clusters compared to other vegetation indices. Figure 3 represents the decision tree for each vegetation index, whereas Figure 4 shows the importance of each observation date. The importance was calculated using the following formula, wherein a larger value indicates higher importance of the dependent variable for classification [14].

$$I(j) = \sum_{i=1}^{n \in F(j)} \left(N_p(i) \times G_p(i) - N_l(i) \times G_l(i) - N_r(i) \times G_r(i)\right)$$

where $I(j)$ is the importance for feature j, $F(j)$ is a set of nodes for which a feature j is to be split, $N_p(i)$ is the number of samples at node i, $N_l(i)$ is the number of left node samples among the child nodes of i, $N_r(i)$ is the number of right node samples among the child nodes of i, $G_p(i)$ is the Gini impurity at i, $G_l(i)$ is the Gini impurity of left nodes among the child nodes of i, and $G_r(i)$ is the Gini impurity of right nodes among the child nodes of i. The Gini impurity at node k – $G(k)$ – was calculated from the number of target labels as n, and the proportion of samples with target label i in node k as $p(i)$:

$$G(k) = \sum_{i=1}^{n} p(i) \times \left(1 - p(i)\right)$$

From Figure 4, NDVI observations were sufficient until the first half of August. The observation period for NDRE was optimal from July 13th at the panicle formation period to August 9th at the earing period. sNDRE and CCCI require observation following August. Subsequently, the cluster IDs in the test data were predicted using the training data only for these important observation ranges. The accuracy rates were approximately 96%, 82%, 95%, and 96% for NDVI, NDRE, sNDRE, and CCCI, respectively.

Thus, the important observation ranges for each vegetation index were clarified using a random forest. However, observations from July to September are necessary when using all four vegetation indices considered in this study, so it is important to use only those vegetation indices that match the application.

Table 4

	NDVI	NDRE	sNDRE	CCCI
NDVI	N/A	-0.013	-0.015	-0.149
NDRE	-0.013	N/A	0.267	-0.047
sNDRE	-0.015	0.267	N/A	0.211
CCCI	-0.149	-0.047	0.211	N/A

Spearman Correlation Coefficient

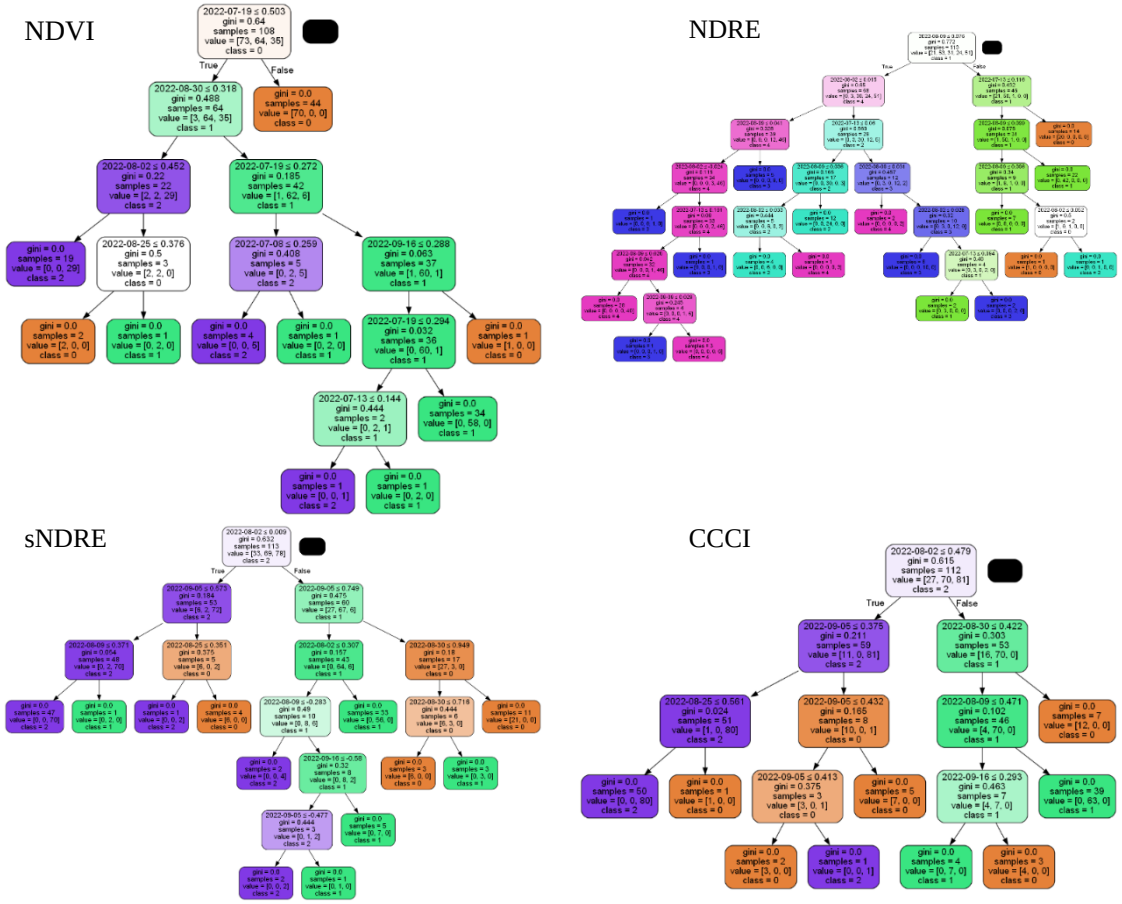

Figure 3: Decision trees for cluster ID classification generated by random forest

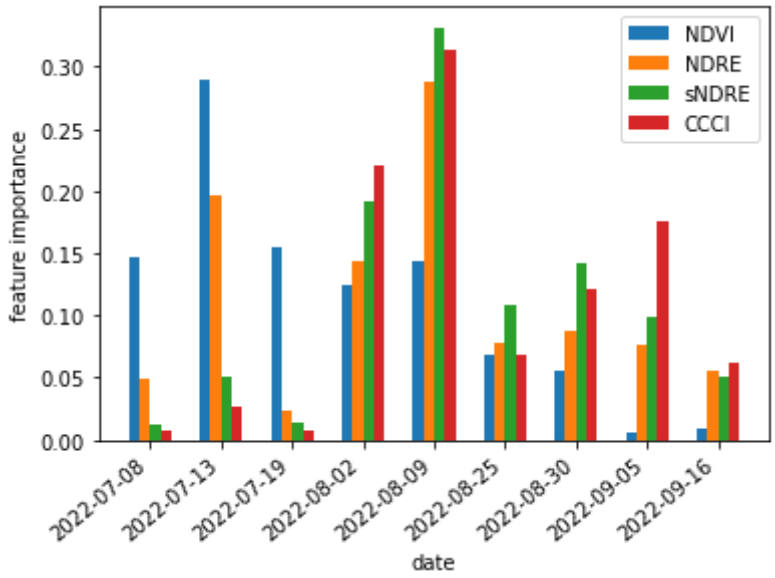

Figure 4: Importance of each observation date

5. Conclusions

In this study, Gramineae crops were continuously monitored with variable fertilizer amounts to evaluate paddy rice and wheat growth by analyzing time-series of multiple vegetation indices. In addition, the periods and locations of crops under stress were visualized along with the nitrogen amount in conjunction with the index values. These results can be used as references to ensure efficient fertilization from the perspectives of the environment and SDGs.

Although valid observation dates were revealed from the importance of dependent variables using the random forest, this importance is relative within each vegetation index. One method to address this problem may be regression of the cluster IDs by a generalized linear model [20], such as multinomial logistic regression, to determine statistically and quantitatively effective observation dates. In the future, we plan to predict cluster IDs with higher accuracy and fewer independent variables using these models. Thus, we expect to quantitatively interpret the important observation ranges to support the conservation of labor in agriculture.

References

[1] K. Tanaka, A. Kondoh, Mapping of Rice Growth using Low Altitude Remote Sensing by Multicopter, Journal of The Remote Sensing Society of Japan 36 (2016) 373-387. doi: 10.11440/rssj.39.S1.

[2] K. Tanaka, Current Status and Challenges of Monitoring | Paddy Monitoring by Drone, 2017. URL: https://dronerice.jp/2017/04/27/. (in Japanese)

[3] Y. Kaneta, M. Nishida, F. Takakai, T. Sato, New growth diagnosis standards of high-yielding rice and demonstration of high yielding using NDVI by GreenSeeker handheld crop sensor, Japanese Journal of Soil Science and Plant Nutrition 91, 6 (2020) 417-425. (in Japanese)

[4] K. Harashina, K. Yamamoto, M. Maki, Y. Muto, E. Kurashima, Monitoring Growth of Water-seeded Rice in Tsunami-stricken Paddy Fields Using UAV-mounted Multispectral Sensor, Journal of Japanese Society of Irrigation, Drainage and Reclamation Engineering 87, 2 (2019) 121-126. (in Japanese)

[5] T. Ito, K. Minamino, S. Umeki, Farm Works Evaluation by Time Series Clustering of Drone Rice Monitoring Data, in: Proceedings of the 84th National Convention of IPSJ 1, IPSJ, Tokyo, Japan, 2022, pp. 829-830. (in Japanese)

[6] S. Umeki, Report on Agriculture-Industry Collaboration in FY2020 and Future Prospects, in: Symposium of Iwate University Research Center for Industrial Science Technology in FY2020:

Agriculture, Engineering, and Food of High Technology: Applications and its Collaboration, Research Center for Industrial Science and Technology, Iwate University, Iwate, Japan, 2021, pp. 67-94. (in Japanese)
[7] G. Fitzgerald, J. Glenn, and D. Rodriguez, G. O'Leary, Measuring and predicting canopy nitrogen nutrition in wheat using a spectral index -The canopy chlorophyll content index (CCCI), Field Crops Research 116, 3 (2010) 318-324. doi:10.1016/j.fcr.2010.01.010.
[8] D. Cammarano, G. Fitzgerald, B. Basso, G. O'Leary, D. Chen, P. Grace, C. Fiorentino, Use of the Canopy Chlorophyl Content Index (CCCI) for Remote Estimation of Wheat Nitrogen Content in Rainfed Environments, Agronomy Journal 103, 6 (2011) 1597-1603. doi: 10.2134/agronj2011.0124.
[9] T. Ito, K. Minamino, S. Umeki, Analysis of Vegetation Indices by Time Series Clustering of Drone Rice Monitoring Data, in: 3rd International Symposium on Electrical, Electronics and Information Engineering (ISEEIE 2023), 2023 (in press).
[10] S. Suzuki, T. Ito, S. Umeki, K. Minamino, Growth Analysis of Wheat by Time Series Clustering of Drone Monitoring Data using Vegetation Indexes, in: Proceedings of the 85th National Convention of IPSJ 1, IPSJ, Tokyo, Japan, 2023. (in Japanese)
[11] Sklearn.ensemble.RandomForestClassifier — scujut-learn 1.2.2 documentation. URL: https://scikit-learn.org/stable/modules/generated/sklearn.ensemble.RandomForestClassifier.html.
[12] Graphviz — graphviz 0.20.1 documentation. URL: https://graphviz.readthedocs.io/en/stable/.
[13] PyDotPlus Homepage — PyDotPlus 2.0.2 documentation. URL: https://pydotplus.readthedocs.io/.
[14] The Mathematics of Decision Trees, Random Forest and Feature Importance in Scikit-learn and Spark. URL: https://towardsdatascience.com/the-mathematics-of-decision-trees-random-forest-and-feature-importance-in-scikit-learn-and-spark-f2861df67e3.
[15] tslearn.clustering.TimeSeriesKMeans — tslearn 0.5.3.2 documentation. URL: https://tslearn.readthedocs.io/en/stable/gen_modules/clustering/tslearn.clustering.TimeSeriesKMeans.html.
[16] A. Ohsumi, R. Morioka, M. Ebato, H. Nakagawa, H. Yoshida, Difference between Attainable Yield and Farmers' Actual Yield in Rice in Japan, in: Proceedings of the Crop Science Society of Japan 91, 1, Crop Science Society of Japan, Tokyo, Japan, 2022, pp.28-38. doi: 10.1626/jcs.91.28. (in Japanese)
[17] K. Tatsumi, Crop Phenotype Measurement by Drone and Prediction of Crop Biomass and Yield by Machine Learning, IPSJ Magazine 63, 2, IPSJ, Tokyo, Japan, 2022, pp.76-96. (in Japanese)
[18] S. Shintaro, Y. Yamasaki, T. Onodera, Investigation and Verification for Expansion of Paddy Rice Income and Improvement of Taste Value by Drone Monitoring, Farming Mecanization, Shinnorinsha CO.,Ltd., Tokyo, Japan, 2022, pp.11-18. (in Japanese)
[19] M. Kawase, F. Matsuda, Correlation and Correlation Coefficient, Journal of Biology and Engineering, 95, 8 (2017) 494-497. (in Japanese)
[20] T. Matsui, T. Ugata, T. Machimura, A Deveropment of Factor Analyzing and Predicting Model of Abandoned Agricultural Land with Machine Learning Algorithms, Journal of Japan Society of Civil Engineers G(Environment) 70, 6 (2014) II_131-II_139. doi:10.2208/jscejer.70.II_131. (in Japanese)